Quantum Melting of the Hole Crystal in the Spin Ladder of $Sr_{14-x}Ca_xCu_{24}O_{41}$

A. Rusydi,[1,2,*] P. Abbamonte,[1,3] H. Eisaki,[4] Y. Fujimaki,[5] G. Blumberg,[6] S. Uchida,[5] and G. A. Sawatzky[7]

[1]*National Synchrotron Light Source, Brookhaven National Laboratory, Upton, New York, 11973-5000, USA*
[2]*Materials Science Centre, University of Groningen, 9747 AG Groningen, The Netherlands*
[3]*Physics Department and Frederick Seitz Materials Research Laboratory, University of Illinois, Urbana, Illinois, 61801, USA*
[4]*Nanoelectronics Research Institute, AIST, 1-1-1 Central 2, Umezono, Tsukuba, Ibaraki, 305-8568, Japan*
[5]*Department of Superconductivity, University of Tokyo, Bunkyo-ku, Tokyo 113, Japan*
[6]*Bell Laboratories, Lucent Technologies, Murray Hill, New Jersey, 07974, USA*
[7]*Department of Physics and Astronomy, University of British Columbia, Vancouver, B.C., V6T-1Z1, Canada*

(Received 12 January 2006; published 7 July 2006)

We have used resonant soft x-ray scattering to study the effects of discommensuration on the hole Wigner crystal (HC) in the spin ladder $Sr_{14-x}Ca_xCu_{24}O_{41}$ (SCCO). As the hole density is varied the HC forms only with the commensurate wave vectors $L_L = 1/5$ and $L_L = 1/3$; for incommensurate values it "melts." A simple scaling between L_L and temperature is observed, $\tau_{1/3}/\tau_{1/5} = 5/3$, indicating an inverse relationship between the interaction strength and wavelength. Our results suggest that SCCO contains hole pairs that are crystallized through an interplay between lattice commensuration and Coulomb repulsion, reminiscent of the "pair density wave" scenario.

DOI: 10.1103/PhysRevLett.97.016403 PACS numbers: 71.20.Be, 71.45.Lr, 73.20.Qt, 78.70.Ck

The two-leg "spin ladder" was introduced [1] as a computationally more tractable version of the *t-J* model believed to be relevant to high temperature superconductivity. Depending upon the parameters chosen, a doped ladder can exhibit either exchange-driven superconductivity [1,2] or an insulating "hole crystal" (HC) ground state in which the carriers crystallize into a static, Wigner lattice [1,3,4]. The competition between these two phases is similar to that believed to occur between ordered stripes and superconductivity in two dimensions [5]. For this reason, the spin ladder is an important reference system in the overall understanding of copper oxides.

An example of a doped spin ladder material is $Sr_{14-x}Ca_xCu_{24}O_{41}$ (SCCO), which for $x > 10$ was shown remarkably to exhibit superconductivity under pressure [6,7]. There is now evidence from transport [8,9], Raman scattering [9,10], and resonant x-ray scattering [11] that under ambient conditions the holes lie in the competing crystallized state, i.e., form a "hole crystal" (HC). At $x = 0$ this HC was shown [11] to be commensurate at all temperatures. This contrasts with the behavior of most Peierls charge density waves (CDWs) in which the wavelength typically shifts and becomes commensurate only at low temperatures [12]. This raises the question of what role commensuration plays, in general, in the physics of a Wigner crystal (WC).

Commensuration effects on a WC were originally considered by Hubbard [13], in the context of one-dimensional polymers, who showed that a WC is most stable when the carrier density is a rational fraction and its wavelength commensurate with the lattice. Excess carriers were postulated to form topological defects or "solitons" [13–15] which carry fractional charge. At a sufficient degree of incommensurability the WC becomes unstable and melts. This "incommensurate melting" is driven by the electron kinetic energy so is qualitatively different from discommensuration effects exhibited by a Peierls-type CDW [12]. To investigate how discommensuration influences the HC in a two-leg ladder, we have used resonant soft x-ray scattering (RSXS) [16–21] to study SCCO as a function of doped hole density, δ.

SCCO is an adaptive misfit material consisting of chain and ladder subsystems with incompatible periods $\sqrt{2}c_c \approx c_L = 3.90$ Å. The misfit results in a buckling along the c axis, sometimes interpreted as a unit cell, with period $c \approx 10c_c \approx 7c_L$, though the period is frequently noninteger [22]. A CDW was reported in the chain layer [23–26], though further examination has raised suspicion that this effect is related to the buckling [27,28].

SCCO is self-doped with 6 holes per formula unit, most of which reside in the chain because of its lower Pauling electronegativity. At $x = 0$ approximately five of the six holes reside in the chain [29–31]. Substitution of Ca for Sr transfers holes from the chain to the ladder [29–31], though the magnitude of this transfer is unclear. X-ray absorption measurements [29] suggest that δ for the ladder ranges from 0.057 for $x = 0$ to 0.079 for $x = 12$. Optical conductivity studies suggest a range from 0.07 to 0.2 [30] while ^{63}Cu NMR studies suggest a range 0.07 to 0.25 [31]. The lack of consensus poses a problem for an x-dependent study of SCCO. However, it is agreed that the transfer is linear in x and we will show that much can be learned using this fact alone.

Single crystals of $Sr_{14-x}Ca_xCu_{24}O_{41}$ (SCCO) with $x = 0$, 1, 2, 3, 4, 5, 10, 11, and 12 were grown by high-pressure floating zone techniques. Crystals were cut with a wire saw and polished with diamond film down to a grit of 0.05 μm. RSXS measurements were carried out on beam line X1B at

the National Synchrotron Light Source with a ten-axis, ultrahigh vacuum-compatible diffractometer. Our momentum resolution was 0.00469 Å^{-1} at the OK edge and 0.00827 Å^{-1} at the Cu$L_{3/2}$ edge. Momenta are denoted with Miller indices of the ladder, i.e., (H, K, L_L) denotes a momentum transfer $\mathbf{Q} = (\frac{2\pi}{a}H, \frac{2\pi}{b}K, \frac{2\pi}{c_L}L_L)$. Values are normalized for changes in lattice parameters with Ca content, x.

In Ref. [11] we reported that SCCO, for $x = 0$, contains a HC with commensurate wave vector $L_L = 1/5$. Here we report the observation of another HC reflection for $x = 10$, 11, 12 with commensurate wave vector $L_L = 1/3$ (Fig. 1). The higher wave vector (smaller period) observed makes sense given the higher values of x and δ. Like the phenomenon at $x = 0$ this reflection breaks the super-space-group symmetry of the composite unit cell [29] so cannot be a reflection from the chain-ladder buckling. Seemingly in contradiction with previous transport and Raman studies [10,32] no hole crystal was observed at any of the intermediate dopings $1 \leq x \leq 5$. The intensity of the HC as a function of Ca content is summarized in Fig. 1. Reminiscent of previous proposals [3,13–15], the HC forms only with commensurate wave vector. The doping is not precisely known but presumably these coincide with rational values of the hole density, δ.

Assuming δ, x and the wave vector L_L are all linearly related Fig. 1 suggests the relationship

$$L_L = 1/5 + 2x/165. \quad (1)$$

From this expression one might expect a HC with wave vector $L_L = 1/4$ to form at $x = 4.125$; however, none is observed. It appears that the HC is stable for odd, though not even, multiples of the ladder period.

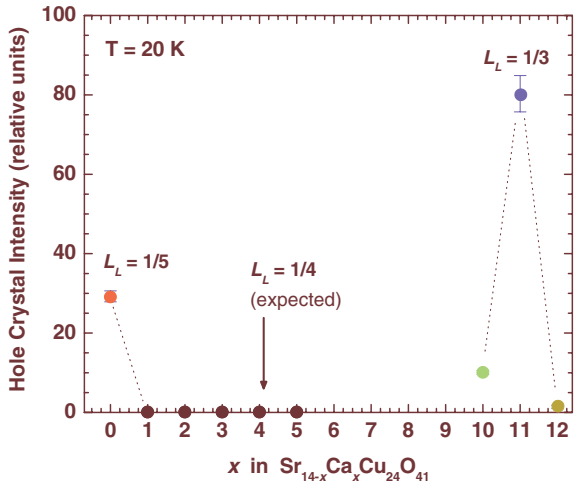

FIG. 1 (color online). Intensity of hole crystal scattering at the OK mobile carrier peak (MCP, 528.6 eV) for all chemical compositions studied. Measurements on different samples were taken at the same beam intensity but were not corrected for absorption or other effects. Symbols are color coded as in Figs. 3 and 4. The dashed lines are a guide to the eye. Hole crystallization occurs only on the rational wave vectors $L_L = 1/5$ and $L_L = 1/3$. No reflection with $L_L = 1/4$ was observed.

The effect of commensurability is seen most clearly in Fig. 2, which shows reciprocal space maps in the $(H, 0, L_L)$ plane around the position $(0, 0, 1/3)$ for $x = 10$, 11, 12 ($T = 20$ K). The maximum HC intensity occurs at $x = 11$ where the wave vector is closest to 1/3. As δ is varied the HC shifts slightly from the commensurate position and "melts." These observations demonstrate that commensuration is critical for the formation of this HC and confirm that lattice constraints can stabilize electronic crystallization even at high carrier density [33,34].

One signifier of the stability of the HC is its correlation length, ξ, which is finite in this material because of disorder. ξ is given by the inverse momentum width of the HC reflection, shown in Fig. 2, which gives the value $\xi_{1/3} = (1600 \pm 90)$ Å $\sim 410c_L$ (near our resolution limit). This value should be compared with the $\xi_{1/5} = 255$ Å $\sim 65c_L$ reported at $x = 0$ [11] (ξ is temperature independent in all samples). ξ was seen to be isotropic at all dopings, even at $x = 0$ where the peak is much broader than our resolution. That ξ is larger at larger L_L shows that the interactions which drive the HC to get stronger as the distance between holes decreases.

We turn now to spectroscopic effects. The reflection with wave vector $L_L = 1/5$ reported at $x = 0$ [11] was visible only with the incident x-ray energy tuned to the mobile carrier prepeak (MCP) below the OK edge and the ligand hole sideband of the Cu$L_{3/2}$ edge. This unusual spectroscopic signature was the reason for identifying this phenomenon as a HC. Slightly different effects are seen at $L_L = 1/3$.

In Fig. 3 we display a "resonance profile" (RP)—the intensity of the HC scattering versus incident energy com-

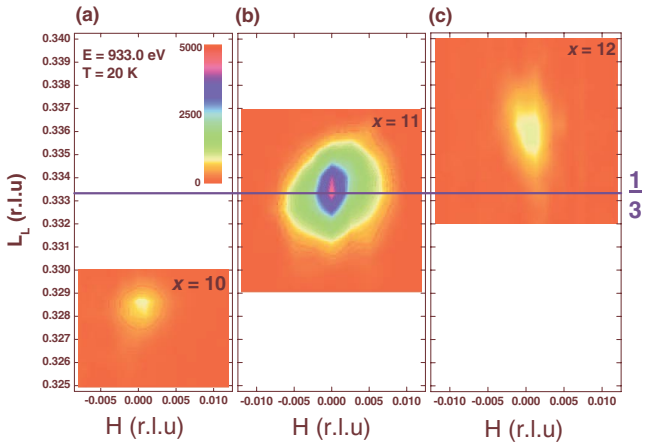

FIG. 2 (color online). Reciprocal space maps around $(H, 0, L_L) = (0, 0, 1/3)$ at the Cu$L_{3/2}$ resonance (photon energy 933 eV) for (a) $x = 10$, (b) $x = 11$, and (c) $x = 12$. The HC is most pronounced when its wave vector has the commensurate value $L_L = 1/3$. As L_L shifts with the addition of carriers the HC melts. All maps were taken with $T = 20$ K.

pared to x-ray absorption spectra (XAS). XAS was taken *in situ* in fluorescence yield mode and is consistent with previous studies [29]. RPs are shown at both edges for $x = 0, 10, 11, 12$. Like the case of $L_L = 1/5$, the $L_L = 1/3$ HC was visible only when the x-ray energy was tuned to oxygen and copper thresholds [11] suggesting a primarily, though not necessarily exclusively, electronic origin [35]. The HC for $x = 10, 11, 12$ resonates at a slightly lower energy than that at $x = 0$ [Fig. 3(a)] due to the well-known redshift of the MCP with increasing doping [36]. Interestingly, the $x = 11$ sample, in which the HC scattering is strongest, also exhibits a second resonance at the OK edge jump at 532.7 eV. This suggests that the hole modulation at $x = 11$ is large enough to modulate the O2p continuum. We did not quantify the hole amplitude but most of the ladder holes are probably modulated at this doping.

New resonant behavior is observed for $L_L = 1/3$ at the Cu$L_{3/2}$ edge. Unlike at $x = 0$, the RP for $x = 10, 11, 12$ consists of two peaks, at 933 eV and 930 eV. The former coincides with the doping-dependent sideband and, like the MCP resonance, indicates the presence of a hole modulation [11]. The latter coincides with the peak of the Cu atomic scattering factor, $f^{ij}_{\mathrm{Cu}}(\omega)$, and indicates a structural distortion in the Cu sublattice. This distortion was not observed at $x = 0$ [11]. The line shape, which exhibits a "dip" in the middle, arises from coherent interference between the two resonances and can be used, in principle, to determine the phase between the hole and structural modulations. Overall, we conclude that the HC at $10 \leq x \leq 12$ is mainly electronic but coupled to the lattice more strongly than at $x = 0$.

The temperature dependence of the HC contains clues about what interactions cause it to form. Figure 4 shows the integrated intensity of the HC peak versus T for $x = 0, 10, 11, 12$. While the $L_L = 1/5$ HC vanishes by $T = 300$ K, the $L_L = 1/3$ HC persists to much higher temperature ($T > 300$ K was not attempted for fear of sample deoxygenation). This indicates, like its larger coherence length, that the interactions driving the HC are stronger at $L_L = 1/3$, i.e., increase with decreasing spacing between holes. If we plot instead the reduced quantities I/I_{20K} and T/τ_{L_L}, where $\tau_{1/3} = 211.1$ K and $\tau_{1/5} = 127.8$ K are the 50% intensity values, the data collapse to a universal curve (Fig. 4, inset). The ratio of the temperature scales $\tau_{1/3}/\tau_{1/5} = 1.65 = 5/3$. In other words, the energy scale of the HC varies inversely with its period. This is evidence that the HC is driven by direct, long-ranged Coulomb repulsion, which one expects in a material in which the carriers are (self-consistently) localized. The importance of direct Coulomb for charge order in correlated systems has been emphasized before [33,34,37] and is also compatible with the HC coherence length, which is isotropic despite the anisotropic crystal structure of SCCO.

It is important to address the relationship between our measurements and the chain charge ordering reported previously [23–28]. We have observed the lowest-order such reflection at $L_L = 0.45$ (or $L_c = 0.31$ in chain units), which was identified as a chain-ladder buckling reflection by Hiroi [22]. This peak has little temperature dependence but has a mixed structure and hole character, suggesting

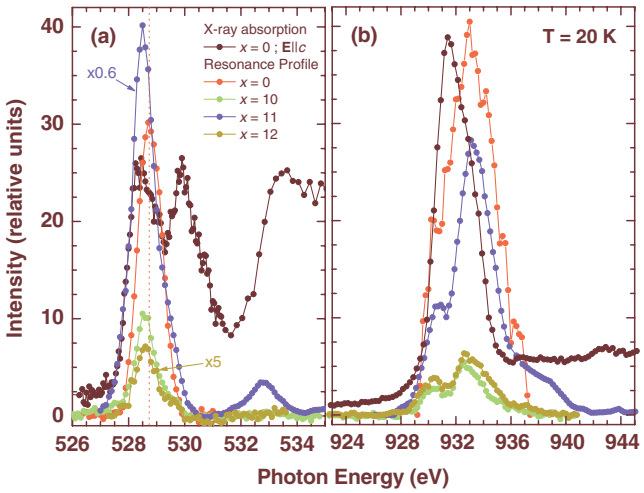

FIG. 3 (color online). "Resonance profiles," i.e., the integrated intensity of HC scattering as a function of incident x-ray energy, compared to x-ray absorption spectra (XAS) of the $x = 0$ system ($\mathbf{E}||c$) near (a) the OK and (b) the Cu$L_{3/2}$ edges. The XAS spectrum is shown in black. Red, green, blue, and brown symbols correspond to $x = 0, 10, 11$, and 12, respectively.

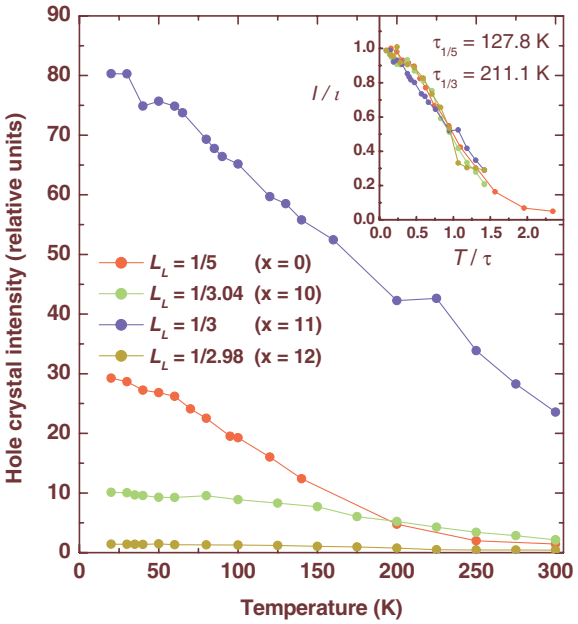

FIG. 4 (color online). Temperature dependence of HC scattering for the four samples in which it has been observed. Red, green, blue, and brown symbols correspond to $x = 0, 10, 11$, and 12, respectively. The data collapse when plotted against the reduced quantities I/I_{20K} and T/τ_{L_L}, where $\tau_{1/3} = 211.1$ K and $\tau_{1/5} = 127.8$ K.

that the chain holes may be pinned in the buckling strain wave.

It is not yet obvious how to reconcile our RSXS results with Raman measurements, which are sensitive to short-range order and reveal HC correlations for all x [10], and impedence measurements, which report long-range HC order for all $x < 9$ [32]. We note, however, that there is close correspondence between the observation of a HC in RSXS and the presence of a metal insulator transition under pressure [7].

In summary, our results indicate that the HC in SCCO forms through an interplay between lattice commensuration and direct Coulomb repulsion, as has been discussed previously [33,34,37]. As discussed in Ref. [11], it is difficult to reconcile the wavelength observed here with the carrier densities determined in Refs. [29,30]; a reexamination of these studies may be necessary. Finally, the absence of a HC with $L = 1/4$ may be due to difficulties with geometrically tiling an even wavelength HC into a plane of edge-shared ladders.

The reader may wonder if there is an inconsistency between the Coulomb interaction apparently at work here and the resonating valence bond (RVB) interaction proposed to drive pairing in spin ladders [1]. That SCCO contains a spin gap at all temperatures is, in fact, strong evidence for paired holes. One possible explanation is that the holes in SCCO are paired but that these pairs are crystallized through Coulomb repulsion and commensuration effects. This would be consistent with the ''pair density wave'' phase proposed to exist in perovskite cuprates [38,39].

We acknowledge helpful input from E. Fradkin, Wei Ku, A. M. Tsvelik, P. Phillips, A. H. Castro-Neto, and S. Fratini. RSXS measurements were supported by the Office of Basic Energy Sciences, U.S. Department of Energy under Grant No. DE-FG02-06ER46285, with use of the NSLS supported under Contract No. DE-AC02-98CH10886. A. R. was partly supported by The Netherlands Organization for Fundamental Research on Matter (FOM). Crystal growth was supported by the 21st Century COE program of the Japan Society for Promotion of Science. G. A. S. was supported by the Canadian Natural Science and Engineering Council, Foundation for Innovation, and Institute for Advanced Research.

*Current address: Institute for Applied Physics, University of Hamburg, D-20335 Hamburg, Germany.

[1] E. Dagotto, J. Riera, and D. J. Scalapino, Phys. Rev. B **45**, 5744 (1992).
[2] M. Sigrist, T. M. Rice, and F. C. Zhang, Phys. Rev. B **49**, 12 058 (1994).
[3] S. R. White, I. Aeck, and D. J. Scalapino, Phys. Rev. B **65**, 165122 (2002).
[4] S. T. Carr and A. M. Tsvelik, Phys. Rev. B **65**, 195121 (2002).
[5] J. M. Tranquada, J. D. Axe, N. Ichikawa, A. R. Moodenbaugh, Y. Nakamura, and S. Uchida, Phys. Rev. Lett. **78**, 338 (1997).
[6] M. Uehara, T. Nagata, J. Akimitsu, H. Takahashi, N. Môri, and K. Kinoshita, J. Phys. Soc. Jpn. **65**, 2764 (1996).
[7] K. M. Kojima, N. Motoyama, H. Eisaki, and S. Uchida, J. Electron Spectrosc. Relat. Phenom. **117–118**, 237 (2001).
[8] B. Gorshunov *et al.*, Phys. Rev. B **66**, 060508(R) (2002).
[9] G. Blumberg, P. Littlewood, A. Gozar, B. S. Dennis, N. Motoyama, H. Eisaki, and S. Uchida, Science **297**, 584 (2002).
[10] A. Gozar, G. Blumberg, P. B. Littlewood, B. S. Dennis, N. Motoyama, H. Eisaki, and S. Uchida, Phys. Rev. Lett. **91**, 087401 (2003).
[11] P. Abbamonte *et al.*, Nature (London) **431**, 1078 (2004).
[12] G. Gruner, *Density Waves in Solids* (Perseus Publishing, Cambridge, MA, 1994).
[13] J. Hubbard, Phys. Rev. B **17**, 494 (1978).
[14] W. P. Su, J. R. Schrieer, and A. J. Heeger, Phys. Rev. Lett. **42**, 1698 (1979).
[15] M. J. Rice, Phys. Lett. **71A**, 152 (1979).
[16] P. Abbamonte, L. Venema, A. Rusydi, G. A. Sawatzky, G. Logvenov, and I. Bozovic, Science **297**, 581 (2002).
[17] H. A. Duur *et al.*, Science **284**, 2166 (1999).
[18] S. B. Wilkins, P. D. Hatton, M. D. Roper, D. Prabhakaran, and A. T. Boothroyd, Phys. Rev. Lett. **90**, 187201 (2003).
[19] S. S. Dhesi *et al.*, Phys. Rev. Lett. **92**, 056403 (2004).
[20] K. J. Thomas *et al.*, Phys. Rev. Lett. **92**, 237204 (2004).
[21] C. Schußler-Langeheine *et al.*, Phys. Rev. Lett. **95**, 156402 (2005).
[22] Z. Hiroi, S. Amelinckx, G. VanTendeloo, and N. Kobayashi, Phys. Rev. B **54**, 15 849 (1996).
[23] M. Matsuda, K. Katsumata, H. Eisaki, N. Motoyama, S. Uchida, S. M. Shapiro, and G. Shirane, Phys. Rev. B **54**, 12 199 (1996).
[24] M. Matsuda *et al.*, Phys. Rev. B **56**, 14 499 (1997).
[25] D. E. Cox *et al.*, Phys. Rev. B **57**, 10 750 (1998).
[26] T. Fukuda, J. Mizuki, and M. Matsuda, Phys. Rev. B **66**, 012104 (2002).
[27] S. van Smaalen, Phys. Rev. B **67**, 026101 (2003).
[28] J. Etrillard, M. Braden, A. Gukasov, U. Ammerahl, and A. Revcolevschi, Physica (Amsterdam) **403C**, 290 (2004).
[29] N. Nucker *et al.*, Phys. Rev. B **62**, 14 384 (2000).
[30] T. Osafune, N. Motoyama, H. Eisaki, and S. Uchida, Phys. Rev. Lett. **78**, 1980 (1997).
[31] K. Magishi *et al.*, Physica (Amsterdam) **403C**, 290 (2004).
[32] T. Vuletić *et al.*, Phys. Rev. Lett. **90**, 257002 (2003).
[33] Y. Noda and M. Imada, Phys. Rev. Lett. **89**, 176803 (2002).
[34] D. Baeriswyl and S. Fratini, J. Phys. IV **1**, Pr1 (2005).
[35] Nonresonant scattering from structural distortions is innately weak in the soft x-ray regime because both the scattering volume and the factor $(\mathbf{Q} \cdot \mathbf{u})^2$ are small. Even considering these two effects, however, the off-resonant scattering here is anomalously weak.
[36] C. T. Chen *et al.*, Phys. Rev. Lett. **66**, 104 (1991).
[37] S. E. Brown, E. Fradkin, and S. A. Kivelson, Phys. Rev. B **71**, 224512 (2005).
[38] Z. Tesanovic, Phys. Rev. Lett. **93**, 217004 (2004).
[39] H.-D. Chen, O. Vafek, A. Yazdani, and S.-C. Zhang, Phys. Rev. Lett. **93**, 187002 (2004).